[Research Paper] 대한금속 · 재료학회지 (*Korean J. Met. Mater.*), Vol. 61, No. 9 (2023) pp.694-703
DOI: 10.3365/KJMM.2023.61.9.694

# Development of Wet Chemical Analysis Technique for Tramp Elements (M = As, Pb, Sb, and Sn) in Silver-M Alloys

**Won-Bum Park[1,†], Yong-Woo Kim[2,†], Sun-Joong Kim[3,*], and Youn-Bae Kang[1,4,*]**

[1]*Graduate Institute of Ferrous and Energy Materials Technology, Pohang University of Science and Technology, Pohang, Kyungbuk, 37673, Republic of Korea*
[2]*Department of Advanced Materials Engineering, Chosun University, Gwangju, 61452, Republic of Korea*
[3]*Department of Materials Science and Engineering, Chosun University, Gwangju, 61452, Republic of Korea*
[4]*Department of Materials Science and Engineering, Pohang University of Science and Technology, Pohang, Kyungbuk, 37673, Republic of Korea*

**Abstract:** Wet chemical analysis techniques for four elements (M = As, Pb, Sb, and Sn) in Ag – M binary alloys were investigated with emphasis on the choice of solvent acid and the characteristic wavelength used in the ICP-AES (Inductively-Coupled Plasma Atomic Emission Spectrometer) analysis. The elements are representative tramp elements in ferrous scrap. The activity of these elements needs to be increased to remove them efficiently during the molten scrap refining process. The activity of these elements in the molten scrap (molten iron alloy) is usually measured by a chemical equilibration technique with molten Ag. Therefore, performing an accurate and reliable chemical analysis of these elements in the molten iron alloy and the molten Ag alloy is important. Preliminary tests using conventional acids (hydrochloric acid, nitric acid) resulted in unreliable results. In the present study, the proper choice of acids as solvents was investigated for each element M in the Ag-M alloys. Several synthesized Ag-M alloys of known compositions were analyzed using two ICP-AES systems independently, for cross-checking. As and Pb in Ag alloys could be successfully dissolved in the nitric acid-based solution. On the other hand, Sb and Sn in Ag alloys did not dissolve in the nitric acid-based solution completely, leaving some precipitates. It was found that the addition of hydrofluoric acid could resolve this problem. In addition to this, the effect of the mass of the Ag-M alloy and wavelength selection during ICP-AES analysis on the accuracy and the reproducibility were investigated. An optimized procedure for the wet chemical analysis of these elements in Ag-M alloys is reported.

(Received 8 March, 2023; Accepted 19 June, 2023)

**Keywords:** Ag-M (M= As, Pb, Sb, and Sn), tramp element, wet chemical analysis, ICP-AES

## 1. INTRODUCTION

Steel is a high-end strategic material for the future because of its cost-effective nature. [1-5]. Recent trends in the iron and steel market are requiring that greenhouse gas emissions be minimized, including $CO_2$ over the whole production process [6-9]. Government-oriented policies to achieve a carbon-neutral state plan are being applied to all industries, including ironmakers and steelmakers [10-15]. Accordingly, it is urgently necessary to reduce the HMR (Hot Metal Ratio) in basic oxygen steelmaking, which can be accomplished by increasing the amount of ferrous scrap [16-18]. In addition, more active use of electric arc furnaces is expected, using ferrous scrap as the main raw material. As a result, the demand for ferrous scrap is projected to increase significantly [19-21]. Among the various types of ferrous scraps, obsolete scrap will be the majority (900 Mt out of 1300 Mt) [16,22]. It is well-known that various tramp elements exist in obsolete scrap. Once these elements enter molten steel during the steelmaking process, they have a significant unwanted impact on the steel product [23-27].

Conventionally, these tramp elements in the ferrous scrap are removed by preliminary treatments, by shredding, and

Won-Bum Park and Yong-Woo Kim equally contributed to this work.
- 박원범: 박사과정, 김용우: 박사과정, 김선중: 교수, 강윤배: 교수
**Corresponding Author:* Sun-Joong Kim
[Tel: +82-10-6600-5627, E-mail: ksjoong@chosun.ac.kr]
**Corresponding Author:* Youn-Bae Kang
[Tel: +82-10-3303-9489, E-mail: ybkang@postech.ac.kr]
Copyright ⓒ The Korean Institute of Metals and Materials

chlorination in the solid state [28-29]. Once these elements dissolve in the liquid steel, and are distributed into fluxes, they can be evaporated from the liquid steel under different conditions to remove the tramp elements [23,24,30-38]. From a fundamental point of view, removing these tramp elements requires increasing their activity coefficient in the liquid steel, which increases the force driving them out of the steel. Distribution of the tramp elements into lime-based flux has not been effective because the distribution coefficient is too low, on the order of $10^{-3}$ to $10^{-5}$ [31,37].

Another feasible method is the evaporation method. The present authors' research group has elucidated the evaporation kinetics and mechanism of Sn and Cu from liquid iron [32-36]. The evaporation of Sn and Cu was found to be largely affected by the C and S contents in the liquid iron. Also, a kinetic model was developed for the evaporation of As and Sn in the BOF (Basic Oxygen Furnace) process [38]. It was determined that the evaporation of As was also affected by the C content in the liquid iron. The key factor in accelerating the evaporation of the tramp elements from the liquid iron was increasing the activity coefficient ($\gamma_{M(\text{in Fe alloy})}$, (M = As, Pb, Sb, and Sn)) in the liquid iron. Accomplishing this requires an accurate and reliable model and database of the activity ($a_{M(\text{in Fe alloy})}$) – composition ($X_{M(\text{in Fe alloy})}$) relation.

An overview of the present strategy is schematically shown in Fig. 1. A multi-component thermodynamic database for steel containing tramp elements has been developed over the years, to provide an accurate activity coefficient of M, which can be used as fundamental data for the evaporation kinetic model [39]. However, because there is still a lack of data regarding tramp elements, further studies are necessary to predict the thermodynamic behavior (activity) of the tramp elements for future ferrous scrap usage.

One of the ways of measuring the activity of M in a Fe-based alloy is to utilize the chemical equilibrium between the Fe-M alloy and the Ag-M alloy, based on the immiscibility of Fe and Ag. This equilibrium yields:

$$M(\text{in Fe alloy}) = M(\text{in Ag alloy}) \quad (1)$$

$$a_{M(\text{in Fe alloy})} = a_{M(\text{in Ag alloy})} \quad (2)$$

$$\gamma_{M(\text{in Fe alloy})} = \gamma_{M(\text{in Ag alloy})} \times X_{M(\text{in Ag alloy})} / X_{M(\text{in Fe alloy})} \quad (3)$$

For this calculation, it is prerequisite to have the activity ($a_{M(\text{in Ag alloy})}$) – composition ($X_{M(\text{in Ag alloy})}$) relation of the tramp elements in liquid Ag. In addition, an accurate chemical analysis of M content in both phases ($X_{M(\text{in Ag alloy})}$, $X_{M(\text{in Fe alloy})}$) is required. With these data, the activity coefficient of M in the Fe alloy can be obtained [40-43]. Sn is one of the tramp elements, and the present authors also measured the $\gamma_{M(\text{in Fe alloy})}$ utilizing the chemical equilibrium between liquid Fe and liquid Ag [44]. However, a preliminary test gave unreliable chemical analysis results because of residues remaining from the pre-treatment with dilute nitric acid solution ($HNO_3$: $H_2O$ = 1:1), particularly for $X_{Sn(\text{in Ag alloy})}$ obtained by wet chemical analysis using ICP-AES (Inductively Coupled Plasma – Atomic Emission Spectrometer).

Generally, the dissolution of pure silver and silver alloy can be accomplished using a nitric acid solution below 373 K, as in the following reaction [45-47]:

$$Ag + 2HNO_3 \rightarrow AgNO_3 + NO_2 + H_2O \quad (4)$$

When the silver alloy including Sn is dissolved in the nitric acid solution, Sn can be precipitated as metastannic acid ($H_2SnO_3$) by the following reaction [48,49]:

$$3Sn + 4HNO_3 + H_2O \rightarrow 3H_2SnO_3\ (\downarrow) + 4NO \quad (5)$$

The metastannic acid in Reaction [5] is a concentrate commonly used to recover Sn in the integral hydrometallurgical waste processing of printed circuit boards. The formation of Sb residues including $SbO_2$ occurs after the extraction of Pb and Ag during the integral hydrometallurgical processing of e-wastes [50]. This indicates that using the general method of wet chemical analysis with a nitric acid solution to determine the composition of Sn and Sb in Ag alloy is challenging, due to the formation of residues.

On the other hand, an analysis method to determine the composition of Ag brazing filler metals was established by the Japanese Standards Association [51]. In this method, Sn dissolved in Ag alloys can be analyzed by dissolving the Ag alloys with a nitric acid solution, followed by precipitating metastannic acid, titration, and the gravimetric method. While the wet chemical analysis method is quite common for element content analysis, details of the procedure are often missing in the open literature. Furthermore, it is assumed that

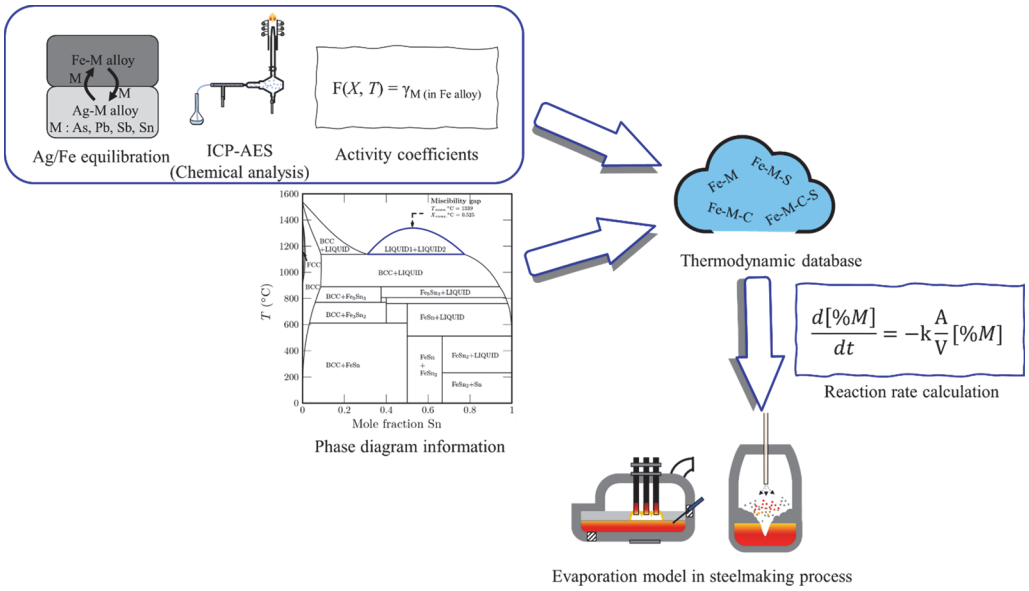


**Fig. 1.** An overview of the present research strategy including the necessity of developing a wet chemical analysis technique.

the residues include a small amount of Ag, which can result in an unreliable determination of Sn contents after the titration and the gravimetric method.

To obtain reliable thermodynamic data about the tramp elements in the Fe phase, it is necessary to accurately analyze the concentrations of the tramp elements in the Ag phase by completely dissolving the sample, without residues such as $H_2SnO_3$ and $SbO_2$. The principle of ICP-AES analysis for measuring the concentration of components in various types of samples that dissolve in an aqua solution is well-known. However, details of the pre-treatments used to make the aqua solution have not usually been disclosed in previous articles. Indeed, many elements in the aqua state have different precipitation reaction characteristics with the mixed acids during the pre-treatment. Therefore, the present authors have attempted to provide details of the pre-treatment, keeping in mind that the tramp elements in the samples (Ag alloys in the present study) might exhibit precipitation reactions with the typical acids used in the pre-treatment, such as $HNO_3$.

The present study investigated the wet chemical analysis technique for various M (= As, Pb, Sb, and Sn) in Ag alloys, with particular emphasis on the choice of solvent acid and the characteristic wavelength for the AES. In order to confirm the validity of the results in a more objective manner, the same analysis was also carried out in two institutes (Pohang University of Science and Chosun University, respectively) with two different sets of equipment. The best-optimized solution treatment and wavelength are reported.

## 2. MATERIALS AND METHODS

### 2.1. Alloy preparation

Several Ag-M (M = As, Pb, Sb, and Sn) alloys of various compositions were prepared in an induction melting furnace. Pure Ag (99.99 pct, DSmetal Corp., Incheon, Korea) was charged in a magnesia crucible (OD 60 mm × ID 50 mm × H 100 mm) and was melted in the furnace. In order to prevent possible oxidation, Ar(g) was dehydrated by passing through a $CaSO_4$ column, deoxidized using Mg chips at 500 °C, and was then flowed in the furnace. After its melting, either a granule or pellet of pure metal M (As, Sn: 99.999 pct, Pb: 99.996 pct, Sb: 99.99 pct, RND Korea Corp., Gwangmyeong-si, Korea) was added to the molten Ag to achieve each target composition (see Table 1). A total 150 g of each was melted in the crucible at 1100 °C for each target composition. The temperature of the melt was checked using a B-type thermocouple which was calibrated with the standard thermocouple (Model C800-65, Type B, 0.5 mm in diameter, 1500 mm in length, CHINO Corp., Tokyo, Japan). The melt was held for 30 min for liquid homogenization and

**Table 1.** Target contents of Ag-M alloys and the wavelength selections for each element in two equipment.

| Elements (M) | Target content (pct) | Thermo Fisher Scientific | Perkin Elmer |
|---|---|---|---|
| | | Wavelength (nm) | |
| As | 1<br>2<br>3 | As 189.042<br>As 193.759 | As 188.979<br>As 193.696<br>As 197.197<br>As 228.812 |
| Pb | 1<br>2<br>2.5<br>3<br>3.6 | Pb 220.383<br>Pb 216.999<br>Pb 261.418 | Pb 220.353<br>Pb 217.000<br>Pb 261.418 |
| Sb | 2.5<br>7.5<br>12.5 | Sb 206.833<br>Sb 217.581<br>Sb 231.147 | Sb 206.836<br>Sb 217.582<br>Sb 231.146 |
| Sn | 2.5<br>5<br>7.5<br>10<br>12.5<br>15 | Sn 189.989<br>Sn 242.949<br>Sn 283.999 | Sn 189.927<br>Sn 235.485<br>Sn 283.998<br>Sn 242.170 |

to minimize possible vaporization of the elements. Small portions of the melt were sampled with quartz tubes $4 \times 10^{-3}$ m in diameter. The surface of the samples was peeled off by a hand grinder and cut into small pieces, of about 0.05 – 0.2 g each, for subsequent solution preparation for the wet chemical analysis.

## 2.2. Solution preparation for Inductively Coupled Plasma Atomic Emission Spectrometry (ICP-AES)

The analysis procedure is illustrated in Fig. 2. All four kinds of alloys weighed approximately 0.1 g and were placed in a Teflon jar. For the Ag-As and Ag-Pb, 10 ml of $HNO_3$:$H_2O$ (1:1) was added. For the Ag-Sb and Ag-Sn, 1 ml of HF in addition to 10 ml of $HNO_3$:$H_2O$ (1:1) was added. Details of the acid selection will be discussed in Section 3.1. These solutions were heated on a hotplate for 2 hrs at 120 – 150 °C. Subsequently, each solution was cooled down to room temperature and poured into a 100 ml flask filtered with filter paper (No. 5C, thickness: 0.22 mm, ADVANTEC Toyo Kaisha, Ltd., Tokyo, Japan). The solutions were left for an additional 24 hrs to complete the vaporization of the unreacted HF. When [pct M] was higher than 3 in each alloy, the solution was diluted by deionized water in order to match the detection limit of the ICP-AES employed in the present study. Standard solutions (1000 μg/ml, Accustandard, New Haven, CT, USA) were prepared as usual to cover the target compositions in Table 1, by mixing the same acids to create the same chemical environment for each element, the deionized water, and adding the major component of the alloys (Ag, 0.1 g/ml of solutions). These standard solutions were used to construct the calibration curve.

In the present study, two different ICP-AES systems were employed: the Thermo Fisher Scientific (Thermo Fisher

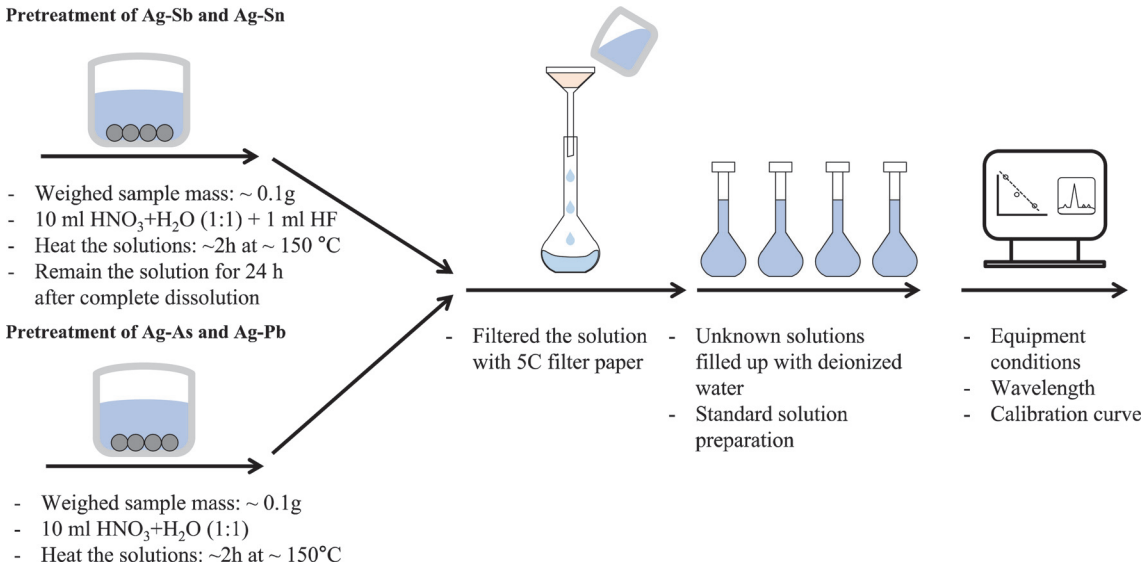


**Fig. 2.** Pretreatment of each Ag-M alloy for the wet chemical analysis.

**Table 2**. Analysis settings for each equipment.

| ICP-AES equipment | Perkin Elmer (Optima 5300 DV) | Thermo Fisher Scientific (ICAP 6500) |
|---|---|---|
| Sample Flow rate (ml/min) | 1.5 | 1.0 |
| Flush Time (sec) | 10 | 30 |
| Delay Time (sec) | 50 | 30 |
| Source equilibration delay (sec) | 19 | - |
| Replicates | 4 | 3 |
| Auxiliary Flow (L/min) | 0.2 | 0.5 |
| Nebulizer Flow (L/min) | 0.2 | 0.4 |
| Power (watts) | 1300 | 1150 |

Scientific ICAP 6500, Waltham, MA, USA) installed at Pohang University of Science and Technology (hereafter referred to as equipment A), and PerkinElmer (Perkin Elmer Optima 5300 DV, Waltham, MA, USA) installed in Chosun University (hereafter referred to as equipment B). The settings are summarized in Table 2.

## 3. RESULTS AND DISSCUSSIONS

### 3.1. Acid selection

As the first step, selected samples of the Ag-M alloys can be put in typical acids such as HCl, $H_2SO_4$, and $HNO_3$. However, it is known that Ag does not dissolve in HCl, and rarely dissolves in $H_2SO_4$ leaving $Ag_2SO_4$ as a precipitate. It was reported that the solubility of $Ag_2SO_4$ was at least twice lower than that of $AgNO_3$, and the solubility of $Ag_2SO_4$ decreased as $Ag^+$ ions increased in solution with $NO_3^-$ ions [52]. Therefore, $HNO_3$ was the first choice for dissolving medium. In the preliminary test, the Ag-Sb and Ag-Sn alloys were first dissolved in the $HNO_3$:$H_2O$ solutions. However, this resulted in precipitation in the solutions. On the other hand, the Ag-As and Ag-Pb alloys dissolved in the same solution without precipitating any residues. Therefore, a mixture of $HNO_3$ and HF was used to dissolve the Ag-Sb and Ag-Sn alloys, as shown in Fig. 2, which will be discussed in Section. 3.2.

### 3.2. Precipitation of Sb and Sn compounds in the solution

Fig. 3(a) shows photographs of the Ag-As and Ag-Pb alloys that were dissolved in the $HNO_3$:$H_2O$ solution. No

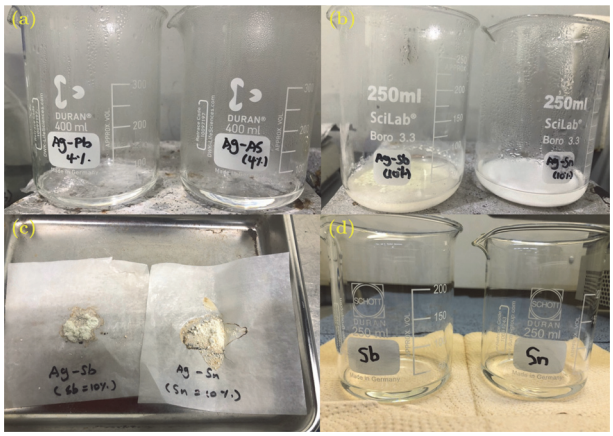


**Fig. 3.** Photographs taken after the acid treatment of Ag-M alloys: (a) Ag-As and Ag-Pb alloys dissolved in 1:1 nitric acid, (b) Ag-Sb and Ag-Sn alloys dissolved in 1:1 nitric acid, (c) precipitates collected after dissolving Ag-Sb and Ag-Sn alloys, which were dried for 1 day, and (d) Ag-Sb and Ag-Sn alloys dissolved in 1:1 nitric acid with hydrofluoric acid.

visible precipitates were observed. However, the dissolved Ag-Sb and Ag-Sn alloys in the $HNO_3$:$H_2O$ solutions left ivory (Ag-Sb) and white (Ag-Sn) precipitates. It was postulated that Sb and Sn reacted with the nitric acid and generated the precipitates (Fig. 3(b) and 3(c)). When Ag-Sb and Ag-Sn alloy was dissolved in the $HNO_3$:$H_2O$ with some amount of HF, no precipitation was observed (Fig. 3(d)).

In order to analyze the precipitates, separate trials were carried out by dissolving a large mass of these alloys in nitric acid. The precipitates were collected with a 5C filter paper and dried at 100 ºC for 1 day. These appeared to be fine powders (Fig. 3(c)). The residues weighed about 1.5 g and were observed using XRD (Bruker, D8-Advance Davinci, Billerica, MA, USA). As seen in Fig. 4, the residues had partial non-crystalline phases with weak peaks. These peaks were matched to $SbO_2$ (Fig. 4(a)) and $SnO_2$, $Sn_6(O_4(OH_4))$ (Fig. 4(b)). Notably, the presence of these precipitates would have caused a noticeable underestimation of the concentrations of Sn and Sb in the Ag alloys.

The results in Section. 3.2 provide evidence why nitric acid cannot be used to dissolve Ag-Sb and Ag-Sn alloys, while Ag-As and Ag-Pb alloys were completely dissolved in the nitric acid without any problem. In order to dissolve the Sb and Sn precipitates completely, HF was used. Several attempts were made in the present study to optimize the

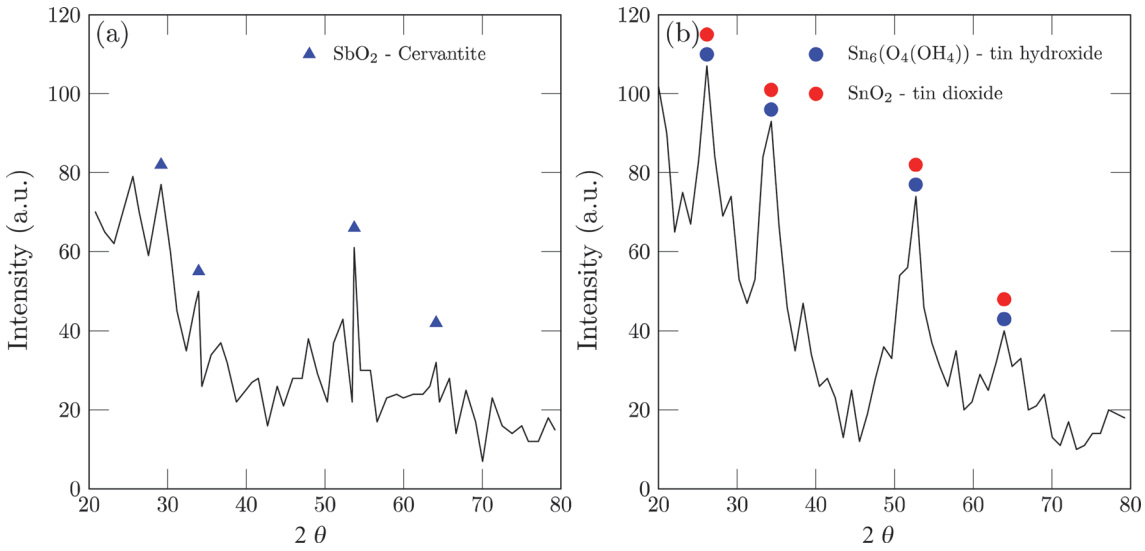


**Fig. 4.** XRD analysis results of the collected precipitates from (a) Ag-Sb alloy and (b) Ag-Sn alloy.

appropriate proportion of HF in the nitric acid solution. When more than 3 ml HF was added to 10 ml $HNO_3$ solution in order to dissolve the Ag-M alloys, a noticeable gas evolution was observed. It probably contained fluorine. The gas evolution continued for 24 hrs at room temperature.

Excess HF added to the $HNO_3$ could remain in the solution, making it unstable, with evaporation. This might produce uncertainties in the analyzed results. Adding less HF to the 10 ml of $HNO_3$ decreased the fluoric gas evolution time to 7 hrs. However, when using less than 1 ml of HF, precipitation occurred. Considering the amount of Ag-Sb and Ag-Sn alloy (about $8\times10^{-4}$ mol for Sb and Sn in 0.1 g) reacting with the HF, 1 ml of HF (about $2.5\times10^{-2}$ mol for $F^-$ in 50 vol% HF 1 ml) is thought to be enough to react with the Sb or Sn solute in the liquid Ag alloy. Therefore, it was concluded that 1 ml of HF mixed with 10 ml of $HNO_3$:$H_2O$ (1:1) to dissolve approximately 0.1 g of Ag-Sb and Ag-Sn alloys was the best option.

### 3.3. Wavelength selection

The prepared aqueous solutions were nebulized into the ICP-AES plasma cores *via* a peristaltic pump. When the excited electron returns to its ground level, electromagnetic radiation is emitted, which is specific to each element. Therefore, the intensity of the radiation should be measured at the corresponding radiation wavelength. While several wavelengths represent an element, the optimum wavelength for the intensity measurement was selected using the following considerations: high intensity and less interference with other elements, in particular with the solvent metal (Ag in the present study). The wavelengths finally selected in the present study are listed in Table 1. Fig. 5 shows the present analysis results for the four elements (As, Pb, Sb, and Sn) at various wavelengths using the two systems (equipment A and equipment B). The contents analyzed by ICP-AES were compared with the target contents calculated using the initial mass of Ag and M melted in the induction furnace.

#### 3.3.1. As

Fig. 5(a) and 5(b) show the analyzed results for As. Reliable analysis results were obtained within ± 5 pct. uncertainty when [pct As] = 1 and 2 in the Ag-As alloys. The agreement was irrespective of the choice of wavelength and equipment. When [pct As] = 3, the analyzed result was somewhat lower than the target composition for both systems. This may be attributed to the vaporization of As in the process of melting the Ag-As alloy, since As passes through sublimation at 614 ºC [53]. Sensitivity due to the choice of different wavelengths was not significant. After considering the intensity of the As peak at each analyzed wavelength, 189.042 nm in equipment A and 188.979 nm in equipment B are recommended to analyze As.

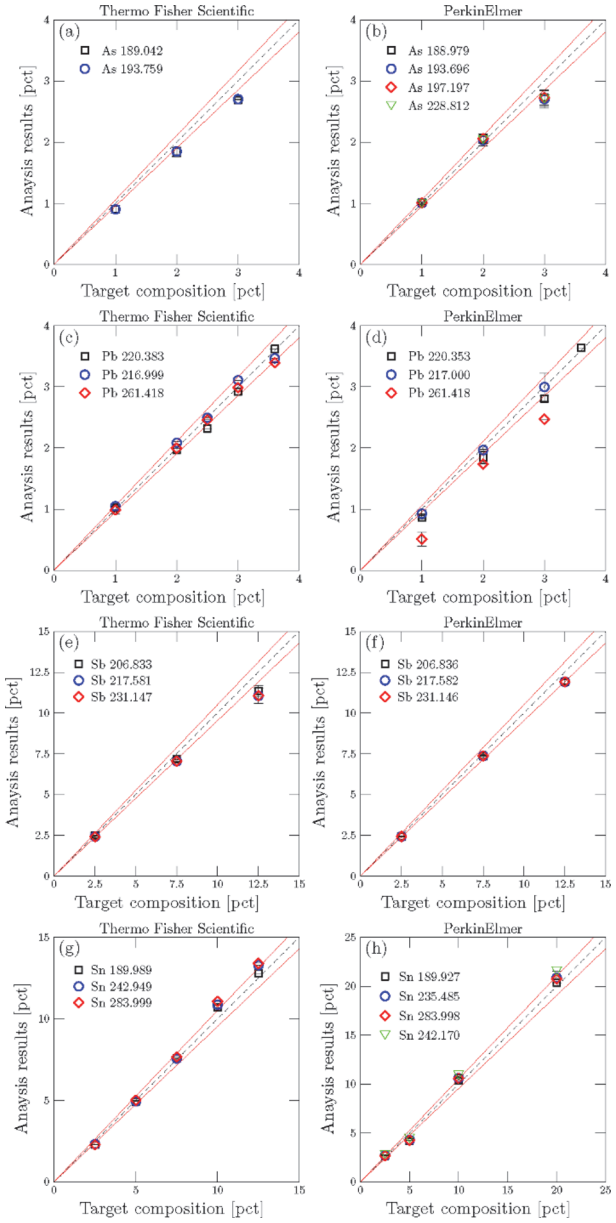


**Fig. 5.** ICP-AES analysis results for (a) and (b) As, (c) and (d) Pb, (e) and (f) Sb, and (g) and (h) Sn.

### 3.3.2. Pb

Fig. 5(c) and 5(d) show the analyzed results for Pb. The results analyzed using equipment B with a wavelength of 217.000 nm showed better agreement with the target contents. Other wavelengths showed noticeable underestimation from the target contents. Analysis reproducibility became lower as [pct Pb] increased. Therefore, it is recommended to use 217.000 nm for the Pb analysis Ag using equipment B. The analyzed results using equipment A were less dependent on the choice of wavelengths. Nevertheless, from the overall agreement assessment, 216.999 nm is most recommended for equipment A to analyze the Pb in the Ag.

### 3.3.3. Sb

Fig. 5(e) and 5(f) show the analyzed results for Sb. Irrespective of the equipment used, the analysis results agreed with the target contents in general. However, when [pct Sb] was 12.5 a slight deviation was found on both equipment. It is to be noted that the present solution (1 ml HF mixed with 10 ml $HNO_3$:$H_2O$ (1:1)) could be successfully used in the analysis of Sb alloyed in Ag, by dissolving the $SbO_2$. The best results were obtained as follows: 206.833 nm for equipment A, 217.582 nm for equipment B for the analysis of Sb in Ag, when [pct Sb] was 7.5 or lower.

### 3.3.4. Sn

Fig. 5(g) and 5(h) show the analyzed results for Sn. A good agreement was obtained with equipment A when [pct Sn] was 7.5 or lower. In the case of equipment B, the analyzed result was in good agreement when [pct Sn] was 5.0 or lower. Unlike the other elements, the analyzed contents of Sn at high [pct Sn] were found to be slightly higher than the target contents. The reason is not clear at present. It is recommended to use 189.989 in equipment A and 189.927 in B, respectively, for the best analysis results.

## 3.4. Sample mass

After analyzing the concentration of Ag-M alloys in this study, it was also confirmed whether there was a relationship between the mass of the specimen used in the analysis and the target concentration. Cases for As and Sb are shown representatively in Fig. 6. Sample masses were in the range of 0.08 – 0.24 g. When the mass of the specimen was more than 0.1 g, the analyzed compositions were in good agreement with the target compositions as shown in Fig. 6. When the target [pct Sb] in Ag was 12.5, the averaged values of contents analyzed by equipment B and equipment A were lower than approximately 0.5 and 1 pct. compared to the target composition, respectively. The melting point and boiling point of pure Sb are 631 ºC and 1587 ºC, respectively [54]. At 1100 ºC, the vapor pressure of liquid Sb is

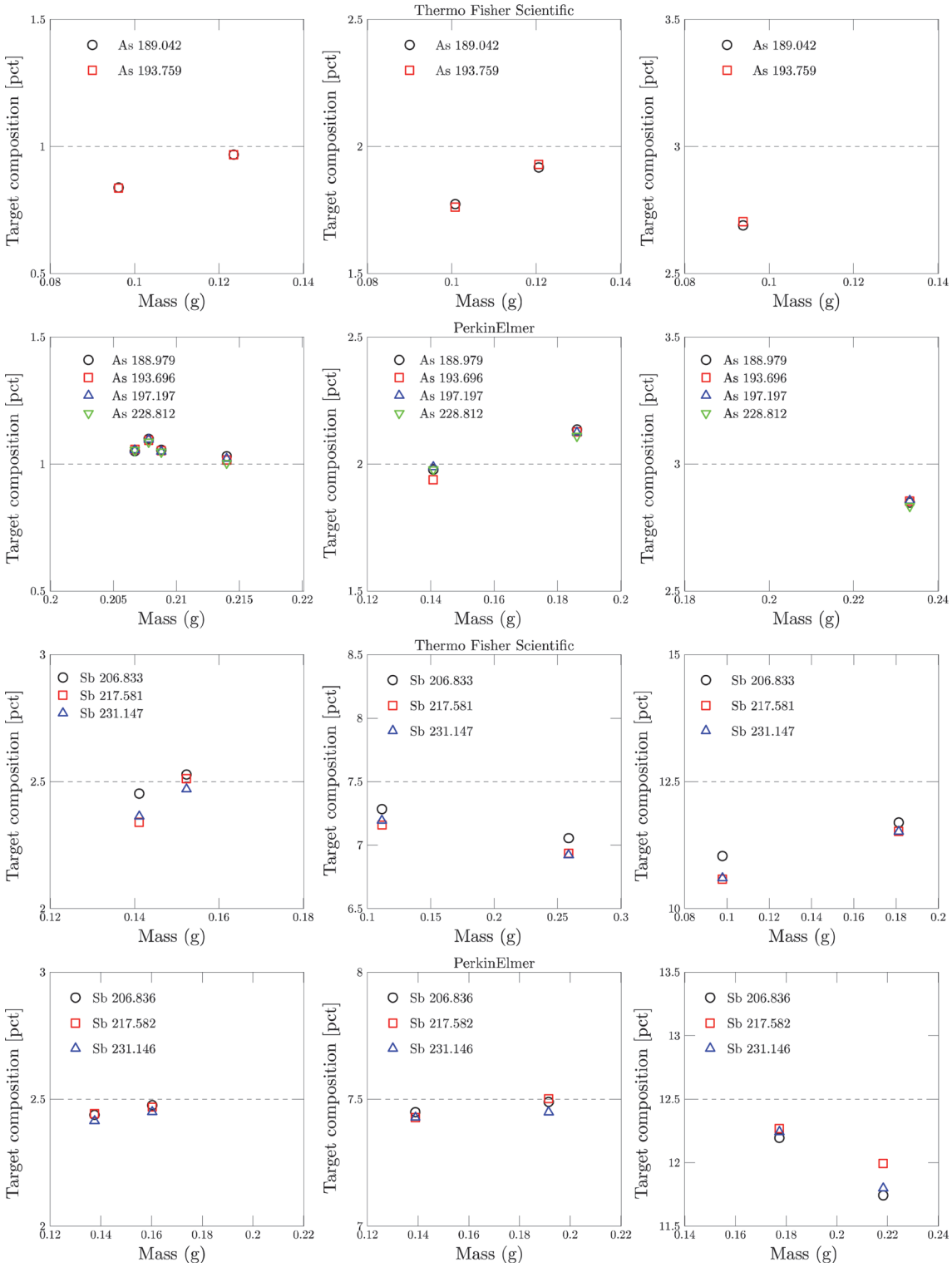


**Fig. 6.** The effect of mass on the target composition in As and Sb.

approximately 0.05 atm. Furthermore, by evaporating Sb oxide, the removal ratio of Sb from the Sb-rich anode slime was reported to be about 90% at 800 ºC [55].

Even though the vapor pressure of Sb in the Ag alloy melts

was not reported, it can be assumed that vaporization of Sb occurred during the melting process used to prepare the high concentration of Sb in the Ag alloy. Therefore, vaporization of Sb caused the slight decrease in the analyzed compositions of Sb in the Ag alloy, compared to the target composition. Consequently, the optimized mass for wet chemical analysis of the Ag alloy sample was more than 0.1 g, and the analyzed concentrations of Sb and As can be lower than the target composition due to vaporization, despite the best choice of wavelength. The vaporization of tramp elements can reduce the contents of tramp elements in ferrous scrap.

## 4. CONCLUSIONS

In the present study, a series of procedures for the wet chemical analysis of tramp elements (M = As, Pb, Sb, and Sn) in Ag alloys were investigated. It was found that the conventional use of $HNO_3$ was fine for As and Pb, but it was problematic for the analysis of Sb and Sn content. An XRD analysis showed that Sb and Sn formed precipitates ($SbO_2$, $SnO_2$, $Sn_6(O_4(OH)_4)$ in the $HNO_3$ solution, which could result in a lower estimation of their contents. The addition of HF to $HNO_3$ solved this problem: 1 ml of HF in 10 ml of $HNO_3$:$H_2O$ (1:1) was used for dissolving 0.1 g of Ag-M alloys.

Two different ICP-AES systems (equipment A: Thermo Fisher Scientific, equipment B: PerkinElmer) were employed to confirm the choice of the acid solution. Moreover, several wavelengths available for each elemental analysis were tested by comparing the target contents of the synthesized Ag-M alloys and the analyzed contents. It was found that not all of the wavelengths could be successfully used for accurate analysis. The following are recommended:

- As: 189.042 nm in equipment A and 188.979 nm in equipment B
- Pb: 216.999 nm in equipment A and 217.000 nm in equipment B
- Sb: 206.833 nm in equipment A and 217.582 nm in equipment B
- Sn: 189.989 nm in equipment A and 189.927 nm in equipment B

It is recommended that a preliminary search be performed for an optimum acid and optimum wavelength available in a given ICP-AES equipment, and will result in improved analysis accuracy.

## ACKNOWLEGEMENT

This research was financially supported by the National Research Foundation of Korea (NRF-2021R1F1A1049973).

## REFERENCES

1. H. An, J. Lee, H. Park, J. Yoo, S. Chung, J. Park, and N. Kang, *Korean J. Inst. Met. Mater.* **59**, 21 (2021).
2. I. Yoo, S.-W. Ko, J. Kim, and B. Hwang, *Korean J. Inst. Met. Mater.* **60**, 102 (2022).
3. M.-G. Jo, S.-H. Ryu, K.-I. Kim, D.-E. Kim, J.-I. Kim, K.-T. Kim, S.-S. Kim, and G.-S. Cho, *Korean J. Inst. Met. Mater.* **60**, 251 (2022).
4. J.-Y. Kim, S.-W. Ko, and B. Hwang, *Korean J. Inst. Met. Mater.* **60**, 811 (2022).
5. H.-S. Kim and J.-J. Kim, *Korean J. Inst. Met. Mater.* **61**, 60 (2023).
6. D. Gielen, D. Saygin, E. Taibi, and J. P. Birat, *J. Ind. Ecol.* **24**, 1113 (2020).
7. M. A. Quader, S. Ahmed, R. A. R. Ghazilla, S. Ahmed, and M. Dahari, *Renew. Sustain. Energy Rev.* **50**, 594 (2015).
8. Á. A. Ramírez-Santos, C. Castel, and E. Favre, *Sep. Purif. Technol.* **194**, 425 (2018).
9. Q. Chen, Y. Gu, Z. Tang, W. Wei, and Y. Sun, *Appl. Energy.* **220**, 192 (2018).
10. Government of the Republic of Korea, *2050 Carbon Neutral Strategy of the Republic of Korea: Towards a Sustainable and Green Society,* http://unfccc.int/sites/default/files/resource/LTS1_RKorea.pdf (2020).
11. J.-Y. Lee, *2050 Long-term Low Carbon Strategy (LEDS) and Steel Industry Challenges,* http://www.kiet.re.kr/research/paperView?paper_no=774 (2022).
12. O. Akashi, T. Hanaoka, Y. Matsuoka, and M. Kainuma, *Energy* **36**, 1855 (2011).
13. The White House, *The Long-Term Strategy of the United States: Pathways to Net-Zero Greenhouse Gas Emissions by 2050*, https://unfccc.int/documents/308100 (2021).
14. J.-H. Bae, K.-M. Kim, K.-U Lee, and J.-W. Han, *Korean J. Inst. Met. Mater.* **59**, 14 (2021).
15. S.-H. Yi, W.-J Lee, Y.-S. Lee, and W.-H. Kim, *Korean J. Inst. Met. Mater.* **59**, 41 (2021).
16. L. Holappa, *Metals* **10**, 1117 (2020).

17. J. Oda and K. Akimoto, *J. Clean. Prod.* **345**, 3 (2022).
18. Q. Zhang, Y. Li, J. Xu, and G. Jia, *J. Clean. Prod.* **172**, 709 (2018).
19. B. Lee and I. Sohn, *JOM* **66**, 1581 (2014).
20. F. Facchini, G. Mossa, G. Mummolo, and M. Vitti, *Energies* **14**, 7395 (2021).
21. M. Sahoo, S. Sarkar, A. C. Das, G. G. Roy, and P. K. Sen, *Steel Res. Int.* **90**, 11 (2019).
22. S. Nicholas and S. Basirat, *New from Old: The Global Potential for More Scrap Steel Recycling*, https://ieefa.org/resources/new-old-global-potential-more-scrap-steel-recycling (2021).
23. X. Zhang, G. Ma, M. Liu, and Z. Li, *Metals* **9**, 834 (2019).
24. S.-H. Sang, *Resour. Recycl.* **29**, 3 (2020).
25. W. T. Nachtrab and Y. T. Chou, *J. of Mater. Sci.* **19**, 2136 (1984).
26. S.?W. Kim and H.-G Lee, *Steel Res. Int.* **80**, 121 (2009).
27. Y. Lan and S. Seetharaman, *Metall. Mater. Trans. B* **42**, 1031 (2011).
28. S.-Y. Lee and H.-S. Sohn, *J. of Korean Inst. of Resources Recycling*, **27**, 54 (2018).
29. F. Tailoka, R. V. Kumar, and D. J. Fray, *Ironmaking Steelmaking*, **30**, 385 (2003).
30. L. Savov, S. Tu, and D. Janke, *ISIJ Int.* **40**, 654 (2000).
31. T. Isawa, T. Wakasugi, K. Noguchi, and N. Sano, *Steel Res.* **58**(7), 296 (1987).
32. S.-H. Jung, Y.-B. Kang, J.-D. Seo, J.-K. Park, and J. Choi, *Metall. Mater. Trans. B* **46**, 250 (2015).
33. S.-H. Jung, Y.-B. Kang, J.-D. Seo, J.-K. Park, and J. Choi, *Metall. Mater. Trans. B* **46**, 259 (2015).
34. S.-H. Jung, Y.-B. Kang, J.-D. Seo, J.-K. Park, and J. Choi, *Metall. Mater. Trans. B* **46**, 267 (2015).
35. S.-H. Jung and Y.-B. Kang, *Metall. Mater. Trans. B* **47**, 2564 (2016).
36. F. Tafwidli, M.-E. Choi, S.-H. Yi, and Y.-B. Kang, *Metall. Mater. Trans. B* **49**, 1089 (2018).
37. D.-H. Kim, Y.-M. Cho, S.-C. Park, S.-Y. Kim, and Y.-B. Kang, *JOM* **73**, 1080 (2021).
38. D.-H. Kim, W.-B. Park, S.-C. Park, and Y.-B. Kang, *Materials* **15**, 4771 (2022).
39. K. Shubhank and Y.-B. Kang, *Calphad* **45**, 127 (2014).
40. F. Tsukihashi, K. Kuroda, S. Arakawa, and N. Sano, *Steel Res.* **65**, 53 (1994).
41. B.-C. Bae and D.-J. Min, *J. of the Korean Inst. Met. Mater.* **36**, 43 (1998).
42. C.L. Nassaralla and E. T. Turkdogan, *Metall. Mater. Trans. B* **24**, 963 (1993).
43. C. Wang, C, T. Nagasaka T, M. Hino M, and S. Ban-Ya, *ISIJ Int.* **31**, 1336 (1991).
44. W.-B. Park, M. Bernhard, and Y.-B. Kang (In preparation).
45. L. Maritinez, M. Segarra, M. Fernandez, and F. Espiell, *Metall. Mater. Trans. B* **24**, 827 (1993).
46. S. K.Sadrnezhaady, E.Ahmadi, and M.Mozammel, *J. Mater. Sci. Technol.* **22**, 696 (2006).
47. J. Schosseler, A. Trentmann, B. Friedrich, K. Hahn, and H. Wotruba, *Metals* **9**, 187 (2019).
48. A. Mecucci and K. Scott, *J. Chem. Technol. Biotechnol.* **77**, 449 (2002).
49. Ž. Kamberovic, M. Ranitovic, M. Korac, Z. Andjic, N. Gajic, J. Djokic, and S. Jevtic, *Metals* **8**, 441 (2018).
50. Y. Ding, S. Zhang, B. Liu, and B. Li, *J. Cleaner Prod.* **165**, 48 (2017).
51. Japanese Industrial Standard JIS Z 3901, Method for Chemical Analysis of Silver Brazing Filler Metals (1988).
52. M. H. Lietzke and R. W. Stoughton, *J. Inorg, Nucl. Chem.* **28**, 1877 (1966).
53. N. A. Gokcen, Bull. Alloy Phase Diagr. **10**, 11 (1989).
54. I. Barin, O. Knacke, and O. Kubaschewski, *Thermochemical properties of inorganic substances, 1st ed*, pp. 617-620, Springer, Berlin, Heidelberg (1977).
55. K. Qiu, D. Lin, and X. Yang, *JOM* **64**, 1321 (2012).